Original Paper

Cellular Physiology and Biochemistry

Cell Physiol Biochem 2011;27:625-636

Accepted: April 12, 2011

A Semi-automated Programme for Tracking Myoblast Migration Following Mechanical Damage: Manipulation by Chemical Inhibitors

Nasser Al-Shanti[1], Steve H. Faulkner[1]*, Amarjit Saini[1], Ian Loram[1] and Claire E. Stewart[1]

[1]School of Healthcare Science, Institute for Biomedical Research into Human Movement and Health (IRM), MMU, Oxford Road, Manchester, *Present address: Loughborough University, Loughborough Design School, Leicestershire

Key Words

Skeletal myoblasts • Muscle injury • PI3 kinase • MAP kinase • Matlab™ • Migration

Abstract

Background: Potential roles for undifferentiated skeletal muscle stem cells or satellite cells in muscle hypertrophy and repair have been reported, however, the capacity, the mode and the mechanisms underpinning migration have not been investigated. We hypothesised that damaged skeletal myoblasts would elicit a mesenchymal-like migratory response, which could be precisely tracked and subsequently manipulated. Methods: We therefore established a model of mechanical damage and developed a MATLAB™ tool to measure the migratory capacity of myoblasts in a non-subjective manner. Results: Basal migration following damage was highly directional, with total migration distances of 948μm ± 239μm being recorded (average 0-24 hour distances: 491μm ± 113μm and 24-48 hour distances: 460μm ± 218μm). Pharmacological inhibition of MEK or PI3-K using PD98059 (20μM) or LY294002 (5μm), resulted in significant reduction of overall cell migration distances of 38% ($p<0.001$) and 39.5% ($p<0.0004$), respectively. Using the semi-automated cell tracking using MATLAB™ program we validated that not only was migration distance reduced as a consequence of reduced cell velocity, but critically also as a result of altered directionality of migration. Conclusion: These studies demonstrate that murine myoblasts in culture migrate and provide a good model for studying responsiveness to damage *in vitro*. They illustrate for the first time the powerful tool that MATLAB™ provides in determining that both velocity and directional capacity influence the migratory potential of cellular movement with obvious implications for homing and for metastases.

Introduction

Skeletal muscle accounts for approximately 45% of total body mass, and is critical for maintaining homeostasis during rest and exercise. It displays a high degree of plasticity and is capable of rapidly responding to stresses associated with growth, maintenance of posture, athletic performance and the repair of injury. In addition to the

KARGER

Fax +41 61 306 12 34
E-Mail karger@karger.ch
www.karger.com

1015-8987/11/0276-0625$38.00/0

Accessible online at:
www.karger.com/cpb

Nasser Al-Shanti
Institute for Biomedical Research into Human Movement and Health (IRM)
School of Healthcare Science,
MMU, Oxford Road, Manchester M1 5GD (UK)
E-Mail n.al-shanti@mmu.ac.uk

requirement for balanced protein synthesis and degradation in the preservation of muscle mass [1], critical roles for skeletal muscle stem cells or satellite cells, which are quiescent myogenic cells originally identified based on their location between the plasmalemma and the basement membrane of muscle fibre[2], in postnatal hypertrophy in response to resistance exercise [3] or e.g. steroid administration [4, 5] and skeletal muscle repair have been reported [6, 7]. Following injury, satellite cells are activated and subsequently migrate to the site of injury, where they fuse with the injured fibre and contribute to its regeneration [7]. Despite this essential role, little is known about the mechanisms by which satellite cells migrate.

By contrast, extensive research has focussed on general cell migration and it is evident that the central mechanism underlying this phenomenon is the dynamic reorganisation of the actin cytoskeleton, which leads to the development of extending protrusions in the direction of cellular migration. These protrusions can be spilt into two distinct types of structure, lamellipodia and filopodia. Lamellipodia are sheet like structures of a cross-linked mesh of actin filaments, whereas filopodia are thinner structures made of parallel bundles of actin filaments [8]. These protrusions are individually connected to the underlying matrix via integrin receptors [9]. Evidently, the ability to control the rate of the actin filament assembly and disassembly is central to effective regulation of cellular migration.

A number of factors, are required to ensure directed migration, including: cell-matrix interactions, chemo-attracting signals from the damaged area and internal biochemical signals orchestrating the directional movement of the cell [10]. These chemo-attracting signals may include the insulin-like growth factors (IGFs), tumour necrosis factor-α (TNF), hepatocyte growth factor (HGF) and other signalling molecules emitted by the damaged tissue and invading white blood cells, following acute injury. The mitogen activating protein kinases (MAPK) and phosphatidylinositol 3-kinase (PI3K) are both centrally involved in cell growth and development and function down stream of several growth factors and cytokines. MAPK is a regulator of gene expression, fat and carbohydrate metabolism, cell proliferation and differentiation, hypertrophy, apoptosis and inflammation [11-16]. It is activated via a wide number of stimuli, including insulin, growth hormone and TNF family, and in contrast to previous research [17] has been shown to couple cellular stress with both adaptive or maladaptive responses in skeletal muscle [18].

The activation of PI3K has a key role in establishing and regulating cell polarity and is also suggested to be a key component involved in cell migration [19]. If cell polarity is compromised, the directed movement of a cell will presumably be compromised, thus having a negative impact on the efficiency of cell migration. Both PI3K and MAPK play important roles in cell proliferation, differentiation and survival, and their inhibition will inevitably lead to a dramatic decrease in cell number and or an increase in cell death. However, the roles that they play in muscle cell migration and injury repair remains unclear. Although PI3K has been widely implicated in influencing cellular movement by the control of cellular extensions, the role of MAPK has largely remained elusive, despite its implicated involvement in a Cdc42-Rac1-MAPK signalling pathway [20]. It is of importance to discover what roles are played by both PI3K and MAPK in cell migration following injury. A greater insight into how these and other potential signalling molecules may influence and regulate damage repair, may allow the future development of pharmacological treatments for degenerative muscle wasting diseases, such as cancer cachexia.

Therefore, we developed a model of injury-induced myoblast migration, which could be tracked using software written in MATLAB and we hypothesised that migration of myoblasts could be manipulated via inhibition of MAP Kinase and PI-3 Kinase signalling pathways. Our aims were therefore to establish a model of skeletal muscle injury *in vitro*, with objectives to: 1) write a MATLAB based image analysis method where the off-line tracking of individual cells would be possible, in order that we could 2) accurately assess cell velocity and directionality; and 3) determine the effects of MAP Kinase and PI-3 Kinase inhibition on muscle cell migration.

Materials and Methods

Materials

All cell culture media and supplements were purchased as sterile or were filter sterilised through a 0.2μM filter. Dulbecco's Modified Eagle's Medium with Glutamax (DMEM/4.5g/l), Heat-inactivated (hi) foetal bovine serum (FBS) and hi new born calf serum (NCS) were purchased from Gibco (Paisley, Scotland); penstrep (penicillin and streptomycin) and trypsin from Bio Whittaker (Wokingham, England); L-glutamine from BDH (Poole, England), gelatin from Sigma (St. Louis, U.S.A). Glassware, distilled water (dH_2O) and phosphate buffered saline (PBS, Oxoid (Hampshire, England)) were autoclaved prior to use. Sterile media was stored at 4ºC and used within one month. Plasticware were purchased sterile from Greiner Bio-one,

(Kremsmunster, Austria) unless otherwise stated. PD98059 (MEK inhibitor) and LY294002 (PI3K inhibitor) were purchased from Calbiochem (Nottingham, England).

Media Composition

Growth Media (GM) composed of DMEM with glutamax was supplemented with 10% FBS, 10% NCS, penstrep, and L-Glutamine, at final concentrations of 1000 $U.ml^{-1}$ and 2mM, respectively. Differentiation Media (DM) composed of DMEM with glutamax supplemented with 2% HS and penstrep (1000 $U.ml^{-1}$) and L-Glutamine (2mM). The reduction of serum allows the cells to undergo spontaneous differentiation and form myotubes, without stimulation by growth factors. All media were stored at 4ºC and used within one month of their composition or were discarded.

Cell Culture

C2 murine skeletal myoblasts, the parental line of C2C12 cells [16] ($1x10^6$ cells/ml) [15, 16] were resuspended in pre-warmed GM and plated onto 0.2% gelatine (Sigma, UK) pre-coated T75 dishes (NUNC) for 10-15 minutes at room temperature, prior to incubation at 37ºC, 5% CO_2 overnight. Following two phosphate buffered saline (PBS) washes, fresh GM was added to the dishes and cells returned to the incubator for 48 h. Upon reaching confluency, GM was aspirated the cells were washed twice with PBS prior to trypsinisation and resuspension in GM for trypan blue (Bio Whittaker, Wokingham, England) cell counting, using a haemocytometer.

Cell Plating and Injury

Cells were dispensed onto pre-gelatinised six-well dishes (NUNC, UK) at a density of $1x10^6$ cells/ml prior to incubation at 37ºC, 5% CO_2 for 48 h, when maximal confluency was reached. Cells were washed twice with PBS, prior to addition of 1ml PBS per well. Damage was incurred via scraping in a unidirectional manner using a plastic scraper to create a clearing free of cells, with dimensions of ~10mm x 5 mm. Wounding protocols, which generated smaller areas of damage as determined utilising the Leica measurement tool (Leica Application Suite Advanced Fluorescence, LAS AF version 2.1.0), or which did not effectively remove all cells from the damaged area (as examined microscopically) were discarded. All wounds were created by one researcher only. PBS was removed and 2ml GM per well added to the cells following 2 further PBS washes. Cells were subjected to live time-lapse microscopy (Leica DMI 6000B imaging system, Leica Microsystems GmbH, Germany) in the absence or presence of specific inhibitors.

Cell Signalling Inhibitor Studies

Cells were grown to full confluency and damaged as described above. To each well 5μM LY294002 (PI3 Kinase inhibitor) or 20μM PD98059 (MEK inhibitor) were added immediately following damage (time 0) and cells were incubated alongside appropriate controls for 48 h. Doses utilised were based on previously optimised doses for these cells [21] . The temporal impact of the inhibitors on migration was also assessed. In these experiments, 5μM LY294002 or 20μM PD98059 were added either at time 0 (as above), or 24 h post damage. The dual effect of MAPK and PI3K inhibition on cell migration following damage was assessed by adding 20μM PD98059 and 5μM LY294002 simultaneously at time 0, experiments were terminated 48 h post damage. Images of cell migration were captured using the Leica CTR600 imaging system (Leica Microsystems GmbH, Germany) every 20min at 10x magnification to create time lapse Audio Video Interleave movies (.avi) of cellular responses using Leica Application suite software, build 1.5.1.

Cell Migration Studies

6 well plates containing damaged cells were placed in the incubator (at 37ºC and 5% CO_2) associated with the Leica microscopy system. Each well was assigned a fixed set of coordinates (in the x, y and z planes) to act as spatial markers in order that repeat images could be captured every 20 min for 48 h. Images at the beginning and the end of filming were assessed to gain average migration distance information. The measurement tool associated with the Leica software enables data to be presented in micrometers as a measure of migration distance. Photomicrographs were obtained at 42 h to capture the apparent migration potential of the cells. These images were stroed in an unmodified form and were also subjected to ImageJ (version 1.44p, National Institute of Health, USA) manipulation in order that the outline of individual cells could be captured and delineated.

Cell Motion Analyses using MATLAB™ as a Tracking Tool

Because the Leica software tool only enables the accurate assessment of forward motion over a given time period, aspects of direction and velocity cannot be acquired. Therefore, in order to more accurately investigate individual cell migration distance, directionality and velocity, a semi-automated cell tracking program was written using MATLAB™ (Version 7.4; The MathWorks) and the Image Processing Toolbox (Version 5.4). For this purpose, original time lapse movies of the cells were transferred from .avi files into a series of frame by frame grayscale images. Using a defined threshold, each greyscale image was converted to binary (black/white) format showing the cells as black. Connected groups of black pixels were labelled using the MATLAB function “bwlabel” and groups of less than 100 pixels were eliminated to remove groups that were not clearly identified as cells. The remaining groups were regarded as potential cells; for each frame, the coordinates of the centroid of each cell were calculated and saved in a .mat file.

The .mat file was further analysed using a second MATLAB™ programme. This program was designed to allow semi-automated tracking of individual cells from frame to frame over 48 h. Analysis of migration was initiated from the frontier of the site of damage e.g. the migration of cells into the wound site. The user is prompted to manually select any cell (labelled group) for tracking in the last frame of the movie (frame χ), the program moves to frame χ -1 and tags the cell nearest to the manually selected one in the previous frame. Whilst viewing the original image upon which the cell location is overlaid, the user is given the option to accept this tag as the same cell, which has moved, or to manually select an alternative tagged

cell, if inappropriate tagging has occurred or if no appropriately tagged cell is offered, to manually select the new location of the cell in the image, therefore visual validation is built into the procedure. This process was repeated for a minimum of ten randomly selected cells per treatment over all frames of the films. A representative figure of the tracking output for 10 individual cells filmed over 48 h is provided (Fig. 1). In addition to the graphics provided for the point by point locomotion of the cells we programmed MATLAB™ to derive 4 additional outputs, key to these experiments: 1) migration distance (unlike the Leica software tool, pixels migrated per frame are the output measure for distance and directionality of migration using Matlab as a tool) of cells in the horizontal plane complete with 95% confidence intervals and mean representation plotted (Fig. 2A), 2) the same graphic representation for vertical migration distance (Fig. 2B). 3) the velocity of any movement in the horizontal and 4) vertical planes (Figs. 2C and 2D, respectively). Validity of the method was assessed by two separate users (inter assay) of the software and by one user (intra-assay) carrying out multiple repeats following its establishment. Three movies and 10 distinct cells per movie were tracked, less than 5 % inter- assay variation was evident and the intra-assay variability was smaller still in terms of cell selection, migration distance, direction and velocity. Consideration was given to comparing Matlab to e.g. Image J as a method of tracking, to check for consistency between software, however, other than by looking at the images and deciding visually whether the cell locations are correctly marked, there is no gold standard for measuring cell locations against which to validate this Matlab script.

Statistics

Data were analysed using Microsoft Excel version 2008 and SPSS version 14 software. Results are presented as the mean ± standard deviation (SD). Statistical significance was determined using one-way analysis of variance with multiple post hoc analyses. Results were considered statistically significant when $P < 0.05$. All experiments were performed at least 3 times in duplicate, unless otherwise stated.

Results

C2 Skeletal Myoblasts are Capable of Migration

We were initially able to successfully establish that incubating cells in a heated/humidified CO_2 chamber associated with the Leica microscope had no adverse effects on cell growth and survival for periods of 48 h when compared with standard incubation conditions. Further, following the damage protocol, C2 cells were capable of migrating towards the origin of damage in the absence of apparent excessive proliferation. Cell movement appeared to occur in a highly directional manner, towards the area of initial damage (Fig. 3Ai & Aii and appendix1 (movie)). Manual assessment of the migration distance suggested that rates of migration were consistent throughout the 48 h of filming (Fig. 3B), with migration distance in both 24 h periods being comparable (0-24 h 491µm ± 113µm; 24-48 h 460µm ± 218 µm).

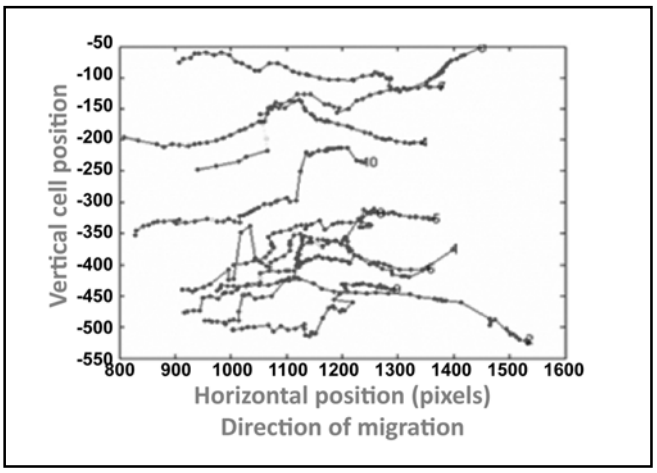

Fig 1. Derived image to illustrate the individual traces of tracked cells on a frame by frame basis using MATLAB™ software. Each blue dot represents the position of an individual cell in a given frame. Green squares demonstrate where cells were not visible and the MATLAB™ program interpolated the cell's movement following the next positive identification of that cell. Cell position on the y axis reflects whether cells were at the top, middle or bottom of the frame. Damage was initiated on the right hand side of the well and cell migration imaged from the left hand side. Frame ÷ in each case is on the far right hand side of the field of view for each selected cell.

Prolonged Activation of PI3 Kinase is Required for Effective C2 Myoblast Migration

Having determined that C2 skeletal myoblasts are capable of migration following damage, rather than simply proliferation or death, we wished to ascertain whether PI3 kinase was influential in this process. Morphologically it appeared that inhibition of PI3 kinase using LY 294002 resulted in a more random and less directed process of migration towards the origin of damage (Fig. 4Ai & Aii). Upon further analysis, it was apparent that inhibition of PI3K with addition of LY294002 at the time of damage (LY-0) resulted in an approximate 50% decrease in migration distance compared control samples (246µm +/- 53µm vs. 491µm +/- 114µm; $p<0.001$; Fig. 4 B). Some recovery in migration distance was evident in the second 24 h period, however the distance was still only 77% of the control migration distance for 24-48 h (354µm ± 73µm vs. 460µm ± 218µm; $p<0.001$; Fig. 4B), culminating in an approximate 38% reduction in total migration distance over 48h (Fig. 4B).

Fig 2. MATLAB™ to assess distance and velocity of migration. A) details the distance travelled by tracked cells in the horizontal plane, with the blue line representing the mean, and the two red lines 95% confidence intervals and the green line representing the exponential curve fit of the data for 10 tracked cells. B) shows the vertical movements of tracked cells; Graph C) tracks the velocity of cells in the horizontal plane, with graph D) detailing the velocity of cells in the vertical plane. Velocity is shown as pixels per frame when using MATLAB™.

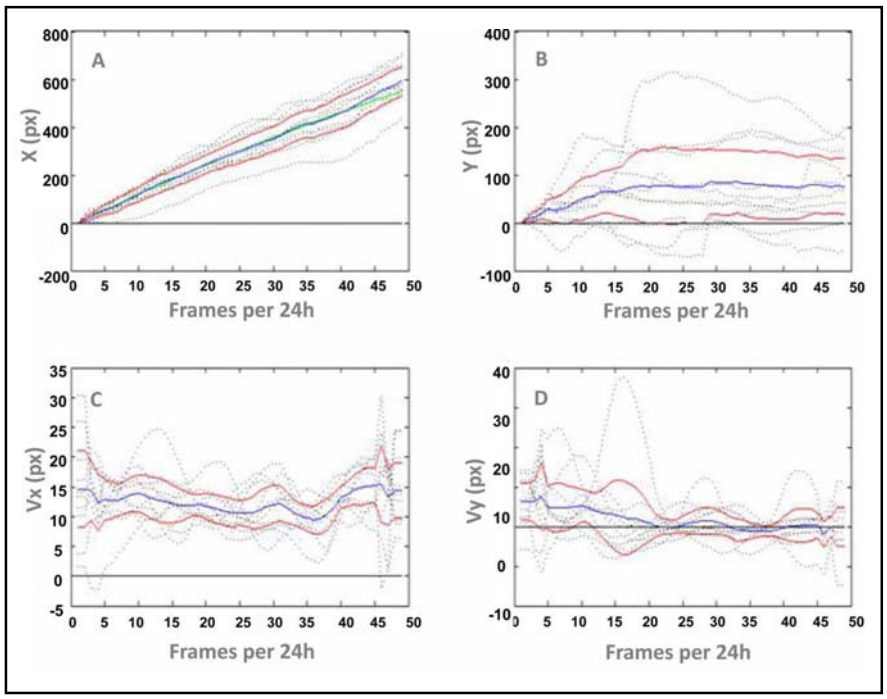

Fig 3. A. Photomicrograph illustration of directionality of cell movement towards the origin of damage (right side of the image). Representative photomicrograph 42 h post damage at 10x magnification is presented in the absence (Ai) or presence (Aii) of ImageJ manipulation. B. Mean migration distance of control cells following damage, illustrating that migration distance was equal for both the first and second 24 h periods following damage. Data shown as mean ± STDEV for a 4 experiments in duplicate.

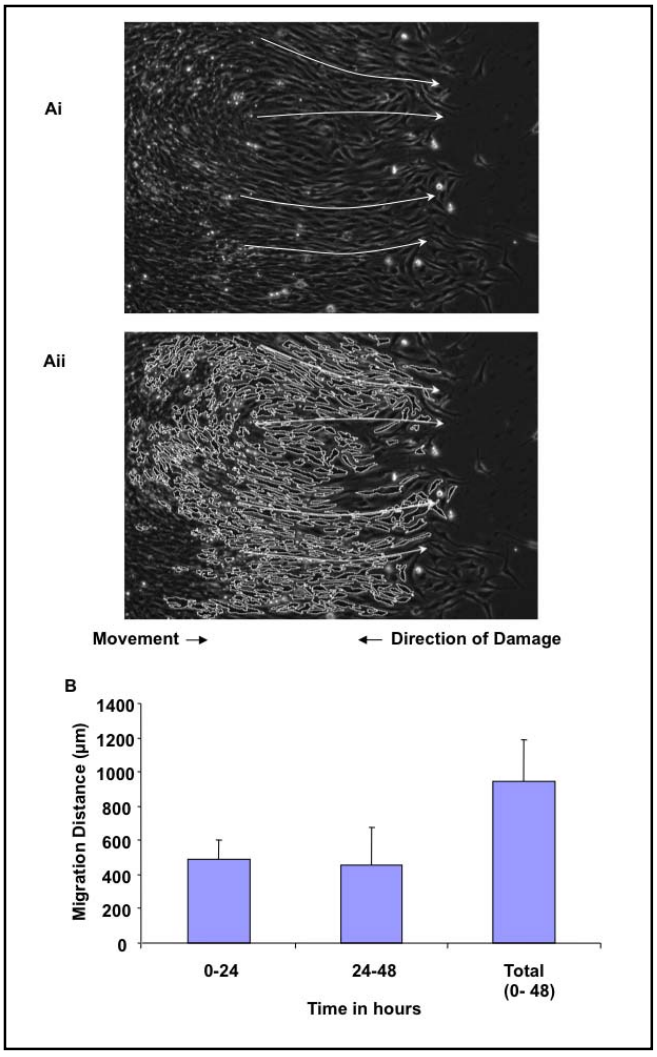

To determine whether PI3 kinase had a persistent regulatory role in migration, or whether it was only required for the initiation of migration, experiments were repeated, but now with a single addition of LY 294002, 24 h following damage (LY-24) and uninhibited cell migration. Critically, this later addition of LY 294002 again resulted in a significant 55% decline in cell migration post inhibitor addition, compared with controls for the 24-48 h time period (210µm ± 12µm vs. 459µm ± 218µm; $p<0.04$; Fig. 4C). Despite uninterrupted migration in the first 24 h, the addition of LY 294002 resulted in a reduction in total migration at 48h of approximately 40% compared with controls ($p<0.001$). Critically no cell death was evident as a consequence of PI3 kinase addition (data not shown) with data illustrating the potent role that PI3 kinase appears to elicit throughout the full 48 h incubation period.

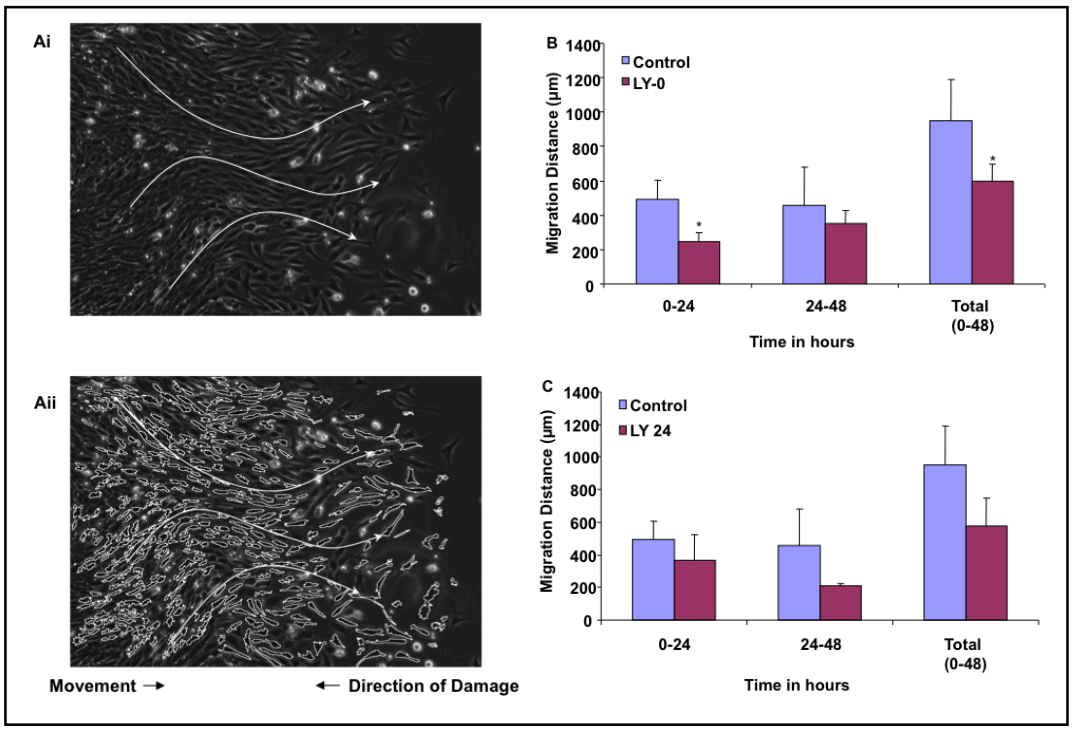

Fig. 4. A. Photomicrograph illustration of reduced directionality of cell movement towards the origin of damage (right side of the image) following LY 294002 (5µM) addition at time 0. Representative photomicrograph 42 h post damage at 10x magnification is presented in the absence (Ai) or presence (Aii) of ImageJ manipulation. B. Mean cell migration following the addition of the PI3K inhibitor LY294002 (5µM) at the time of cell damage. The inhibition of PI3K led to a 50% decrease in the distance of cell migration in the initial 24 h ($p<0.001$), with some recovery in migration distance in the following 24 h although the difference in total migration remained highly significant ($p<0.001$). Data presented as mean ± STDEV of 5 experiments in duplicate. C. Mean cell migration following the addition of LY294002 (5µM) 24 h after damage resulted in a significant decline in 24-48 and 0-48 h migration (*$p<0.04$, **$p<0.01$). Data presented as mean ± STDEV of 3 experiments in duplicate.

Prolonged Activation of MAP Kinase is Required for Effective C2 Myoblast Migration

Having illustrated a critical role for PI3 kinase in myoblast migration, but having determined that migration was not fully blocked, we next wished to determine, whether MAP kinase activation may also be important for myoblast migration. Once again, morphologically it appeared that inhibition of the MEK signalling pathway utilising PD98059 (20 µM) resulted in a more random and less directed process of migration towards the origin of damage (Fig. 5Ai & Aii). Further investigation illustrated that MAPK inhibition (when PD was added at the experimental onset (PD-0)) resulted in an approximate 47% significant decline in cell migration distance over the first 24 h vs. control (262µm ± 110µm vs. 491µm ± 113µm, $p<0.0001$; Fig 5B), respectively. Furthermore, unlike in the presence of LY294002, recovery of migration during the second 24 h period was not as marked, with mean migration distance reaching only 312µm ± 82µm vs. 459µm ± 218µm in control cells ($p<0.03$). Overall migration distance was reduced by 40% to just 573µm ± 170 compared to 950µm ± 331µm for the control samples ($p<0.0004$; Fig. 5B).

Again, wishing to ascertain the potency of the MAP kinase signalling pathway in the second 24 h period, the addition of PD98059 (20µM) 24 h post damage initiation (PD-24) was assessed and resulted in a 42% suppression in cell migration to 269µm ± 22µm (Fig. 5C; $p<0.05$), which was indistinguishable from the inhibition evident when PD98059 (20µM) was added at 0 h (PD-0; Fig. 5B) and which resulted in an approximate reduction in total cell migration of 29% over 48h compared with control samples (Fig. 5C).

MATLAB™ Development for Quantification of Cellular "Kinesiology"

Having determined that myoblasts housed within an external incubator and provided with heat, humidity and 5% filtered CO_2 were capable of survival and migration (as determined using time laps microscopy and simple Leica measuring software), we next demonstrated that migration could be modified by inhibitors of MEK and PI3K. Wishing to validate out data pertaining to cellular movement, a MATLAB™ programme was written, in order to measure not only changes in average migration distance (as determined above), but also in velocity and directionality, key parameters essential for effective wound healing and which could not be assessed using standard Leica software. Initial studies consolidated the measures attained above under control conditions, with

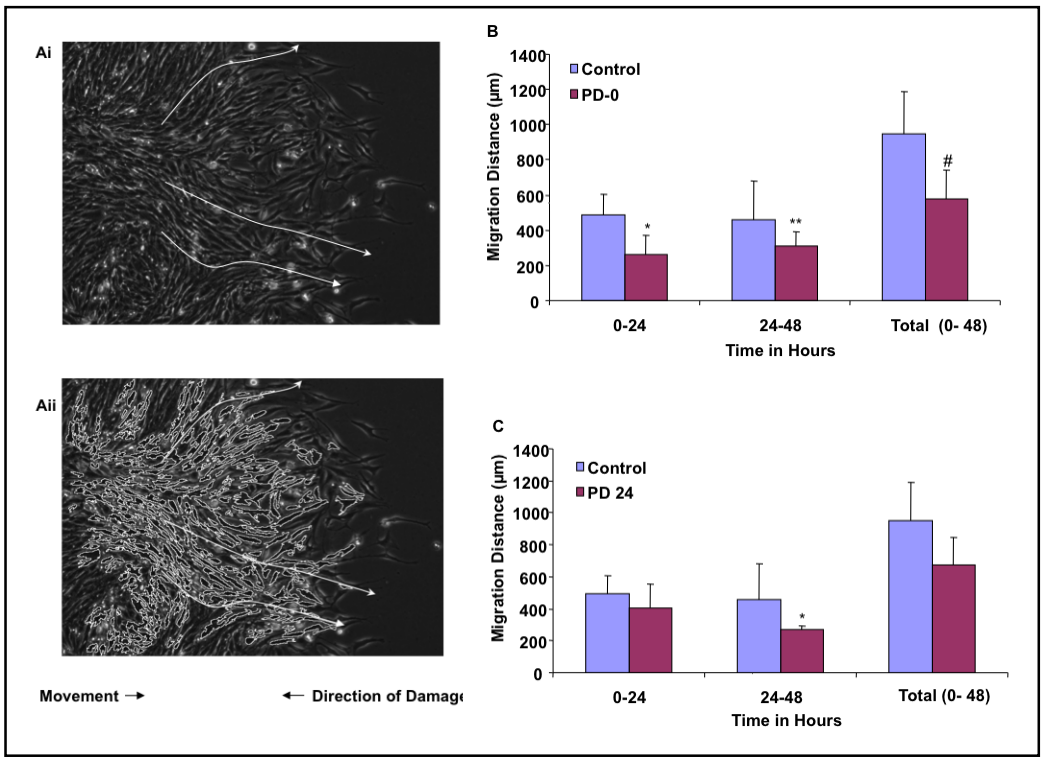

Fig 5. A. Photomicrograph illustration of reduced directionality of cell movement towards the origin of damage (right side of the image) following PD98059 (20µM) addition at time 0. Representative photomicrograph 42 h post damage at 10x magnification is presented in the absence (Ai) or presence (Aii) of ImageJ manipulation. B. Mean cell migration following the addition of the MEK inhibitor PD98059 (20µM) at the time of cell damage. There was a significant reduction in the 0-24 h migration distance (*$p<0.0001$, 261.5µm ± 109.4µm) and very little recovery in migration in the 24-48 h period (**$p<0.04$, 312.2µm ± 81.9µm). Together, this resulted in a significant reduction in migration over the 48 h (#$p<0.0004$). Data presented as mean ± STDEV of 3 experiments in duplicate. C. Mean cell migration following PD98059 (20µM) addition 24 h after damage resulted in a significant 42% decline in migration distance in the second 24 h ($p<0.05$, 268.7µm ± 21.7µm). Data presented as mean ± STDEV of 3 experiments in duplicate.

overall cellular migration (48h) averaging at 819 ± 86 pixels (Fig. 6A). In order to consolidate this finding, measures of horizontal (Figs. 6B +Ci) and vertical (Fig. 6B + Cii) movement and velocity (Figs. 6B + Ciii and 6B + Civ) were performed at 0-24 h (Fig. 6B) and 24 – 48 h (Fig. 6C). These data illustrate a continuous forward (horizontal; x) movement and velocity within each 24 h period. Movement and velocity in the vertical (y) plane, are consistently lower than those seen for forward migration, thus confirming the highly directional movement of the cells under basal injury conditions.

Influence of PI3K and/or MAPK inhibition on cell directionality and velocity

Inhibition of PI3K using LY294002 at the time of damage resulted in disruption of the cellular migration pattern. Figure 7 (A and E) illustrates that over 48h, there was a 50% reduction in horizontal migration distance (461 ± 61 pixels vs. 819 ± 86 pixels, $p<0.0001$) compared with controls (shown in Fig. 6). This reduction was associated not only with a reduction in the velocity of migration (Fig. 7C & G), but critically, in the first 24h, was also associated with increased vertical migration (Fig. 7B) compared with controls, suggesting both slower and more random movement in this period. However, in the second 24h period, the vertical deviation and velocity were virtually 0, (Figs. 7 F & H) suggesting that recovery in directional migration, rather than velocity occurs as a priority in the presence of a single dose of LY treatment.

Inhibition of MAPK signalling pathway at the time of damage resulted in a significant decline in horizontal cell migration over the entire 48 h period (392 ± 40 pixels vs. 819 ± 86 pixels, $p<0.0001$; Fig. 8A & E), when compared with controls (shown in Fig. 6), which was associated with a halving in the migrational velocity of the cells (Fig. 8C & G). Critically and despite first impressions (Fig. 5A) vertical movement and velocity in both the 0-24 h period (Fig. 8B & D) or the 24-48 h time period (Fig 8F &H) were virtually negligent, suggesting that unlike in the presence of LY, MEK inhibition does not alter migration distance through loss of directionality, rather distance is blunted as a consequence of reduced migrational velocity in the horizontal plane for the duration of the experiment.

Finally, wishing to ascertain whether the cells utilise PI3K and MAPK signalling pathways exclusively, we

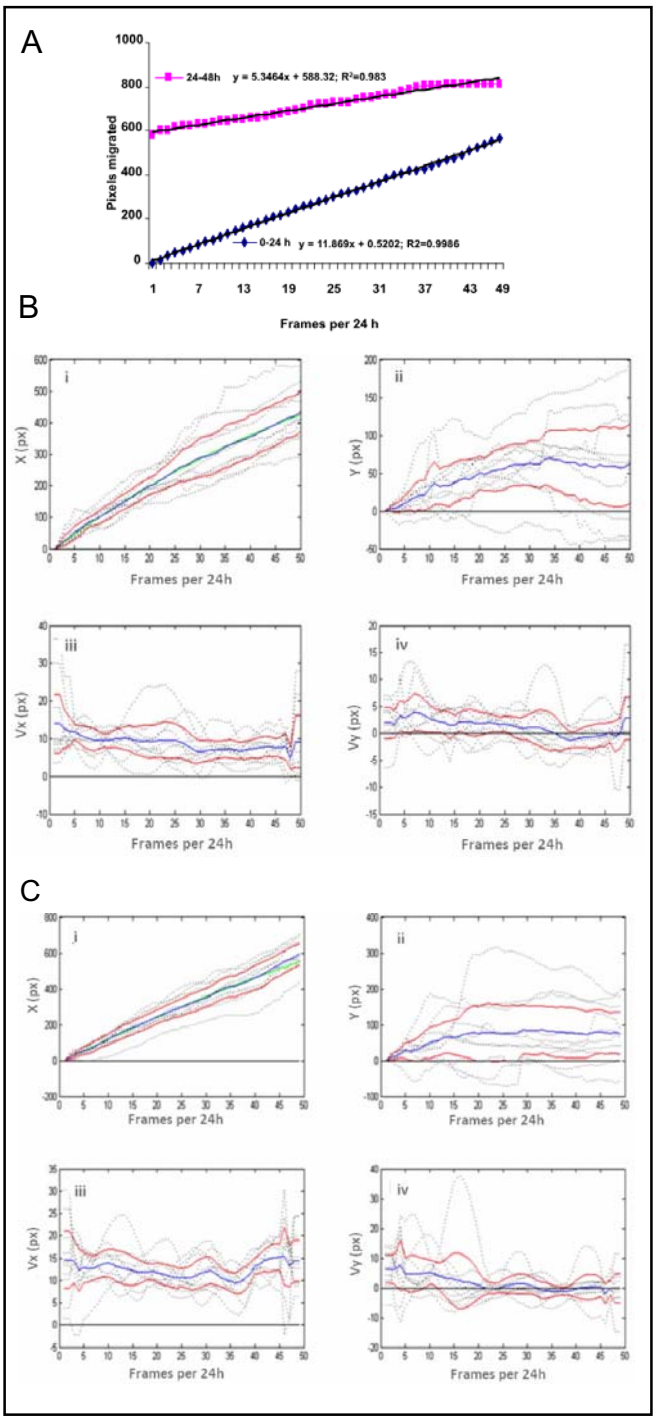

Fig 6. Data depicted demonstrate the average forward migration under control conditions as calculated using MATLAB™ cell tracking over 48 h; A. The data show the mean migration distance from one film (10 cells) to illustrate changes in migration distance over 48 h. MATLAB™ graphs showing the direction (i) and velocity (iii) of cell migration in the horizontal plane and direction (ii) and velocity (iv) in the vertical plane. Graph B represents 0-24 h and graph C 24-48 h. Red lines represent 95% confidence intervals. The blue line is the mean of all tracked cells and the green line representing the exponential curve fit of the data for 10 tracked cells.

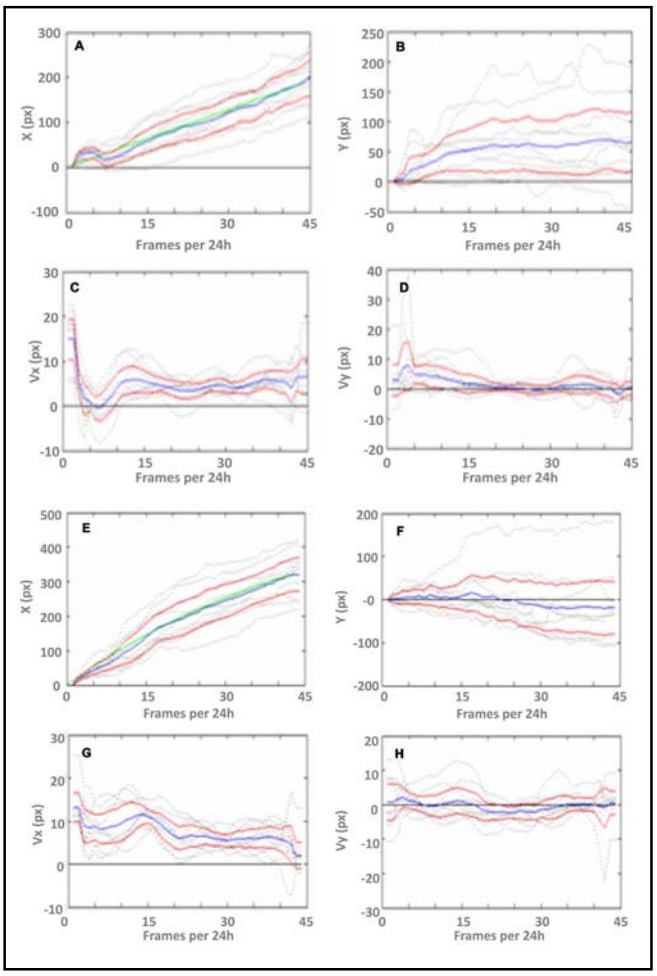

Fig 7. Data depict the effect on migration following PI3K inhibition with LY294002 added at time 0 h. Graphs illustrate the direction of cell migration in the horizontal (A and E), and vertical (B and F) planes. Also shown is the velocity of cell migration in the horizontal (C and G) and vertical (D and H) planes. Graphs A-D represents 0-24 h and graphs E-H 24-48 h. Data represent the mean of 10 tracked cells from a single experiment, for 5 experiments in duplicate. The blue line is the mean of all tracked cells and the green line representing the exponential curve fit of the data for 10 tracked cells.

assessed the impact of blocking both on cellular migration. Critically, inhibition of both pathways did not culminate in cell death. Fig. 9 (A-H) demonstrates the potent effect of dual inhibition of both MAPK and PI3K signalling pathways at the time of damage. Cell migration distance in the horizontal plane was significantly reduced (252 ± 31 pixels vs. 819 ± 86 pixels, $p<0.0001$) compared with control experiments (shown in Fig. 6) over the 48 h incubation period, this reduction in migration distance appears to be underpinned by a reduction in horizontal

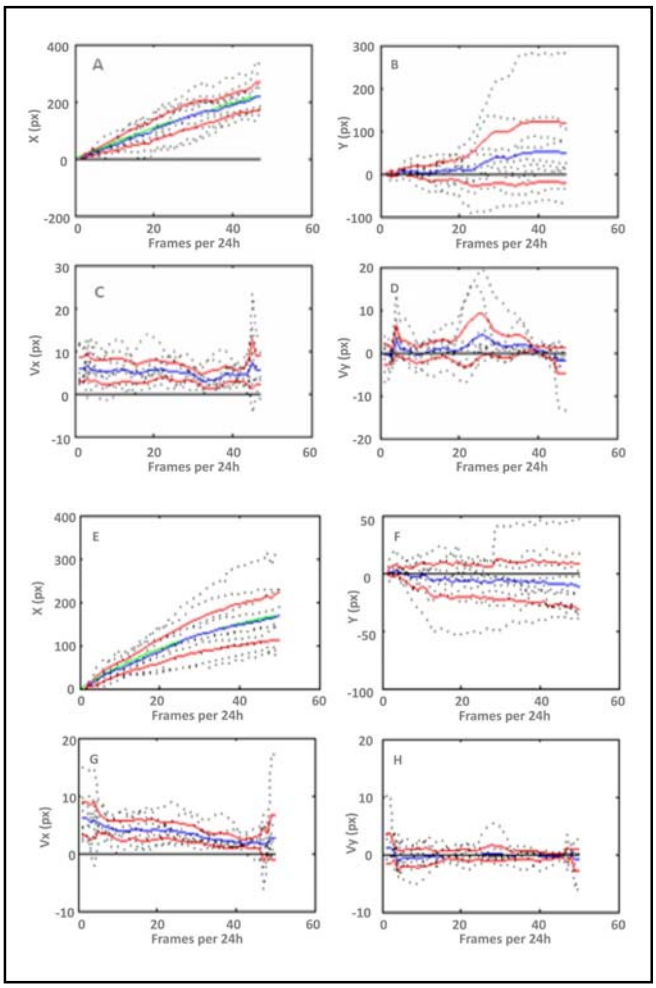

Fig 8. Data depict the effects on migration following MAPKK inhibition with PD 98059 added at time 0 h. Graphs illustrate the direction of cell migration in the horizontal (A and E, and vertical (B and F) planes. Also shown is the velocity of cell migration in the horizontal (C and G) and vertical (D and H) planes. Graphs A-D represents 0-24 h and graphs E-H 24-48 h. Data are representative of the mean of 10 tracked cells from a single experiment, for 3 experiments in duplicate. The blue line is the mean of all tracked cells and the green line representing the exponential curve fit of the data for 10 tracked cells.

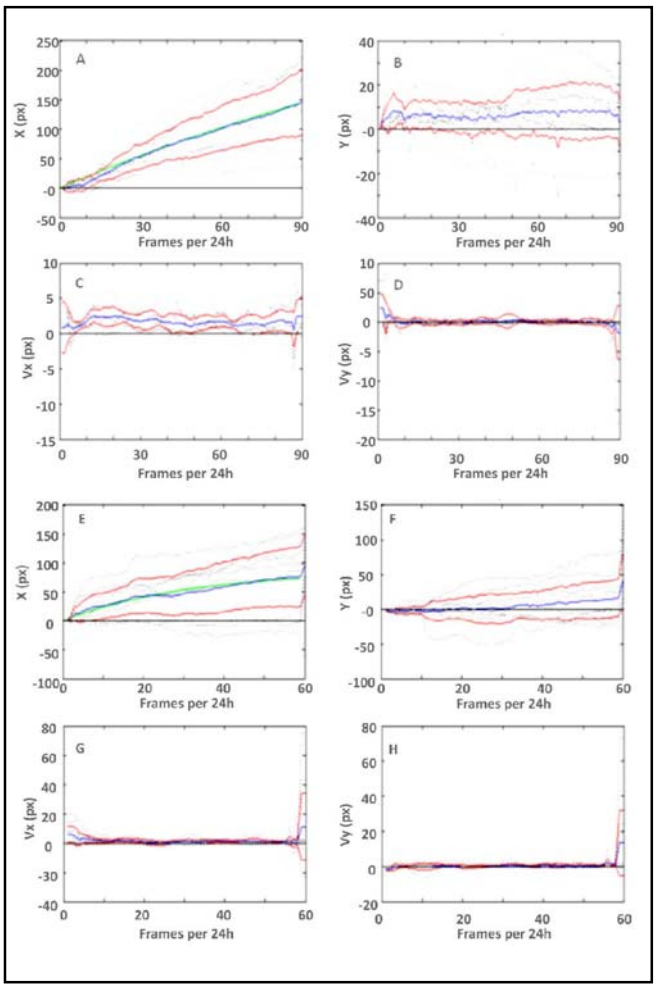

Fig 9. Data depict the effects on migration following dual inhibition of MAPKK and PI3K at time 0 h. Graphs illustrate the direction of cell migration in the horizontal (A and E, and vertical (B and F) planes. Also shown is the velocity of cell migration in the horizontal (C and G) and vertical (D and H) planes. Graphs A-D represents 0-24 h and graphs E-H 24-48 h. Data are representative of the mean of 10 tracked cells from a single experiment, for 3 experiments in duplicate. The blue line is the mean of all tracked cells and the green line representing the exponential curve fit of the data for 10 tracked cells.

migration velocity to 25% of control values (Fig. 9C &G). Critically, the overall decline in migration distance does not appear to be associated with deviation in the vertical plane, since migration distance (Fig 9B &F) and velocity (Fig. 9D & H) approached 0 throughout the study period.

Discussion

We report here, the writing and implementation of a purpose designed MATLAB™ based analytical program for tracking 2-D cell migration following myoblast damage. This methodology was based on previously described script implemented for the automated identification of axonal cones from time-lapse images [22]. The development of such a programme enables accurate assessment not only of cell movement with extended time, but also of overall cell migration distance, direction and velocity, parameters which cannot easily be obtained using live cell imaging alone. It extends current 2-D techniques [23], which are routinely used for monitoring cell migration, and include 1. polarisation assays, which monitor short

term (1-3 h) cellular phenotypes and cell spreading and act as surrogates for migration [24, 25]. 2. wound healing assays, upon which our study is based and which generally track cells for 3 – 24 h to facilitate pharmacological studies, but do not distinguish between proliferation and migration [26]; 3. Boyden chamber or transwell-based assays, designed to monitor the transmigration of cells across physical barriers of varying pore sizes and towards chemoattractants. Short time frames can be applied, but the method does not distinguish between chemotaxis and chemokinesis [27]; and 4. plasma or photo-lithography, which like our method reported here, provide the user (in conjunction with live cell imaging) with the capacity to measure directionally confined cellular migratory distance, velocity and direction [28, 29].

Our live cell imaging, in conjunction with the matlab programme, like the lithography method, provides a simple and reliable method for tracking cell migration, direction and velocity – key features of the wound healing process e.g. if velocity is maintained, but direction is incorrect, cells may actually move away from, rather than towards a site of damage, yet attain a good migration distance. Our reported method differs from the lithography method in that no confinement is placed on the selection of migration "chosen" by the cells in that they have freedom of movement across a large wound area. This provides the capacity to supplement studies with specific chemical inhibitors, as we have done, in order to monitor the impact on homing capabilities following wounding, again, an essential criterion for effective wound closure. We therefore present here a supplementary Matlab script and derived data (Figs 6-9) customised for the specific purpose of tracking cell positions, direction and velocity and therefore prone to little error. The novelty of this is that the Matlab script was customised for the analyses of the captured image sequences, and thus made it possible and easy to record and keep track of individual cells as they moved from frame to frame thus recording their location in a consistent manner. The image processing techniques involving the thresholding into black and white, grouping of contiguous back pixels, calculating centroids and finding the nearest centroids in adjacent frames are not new techniques, however, the usefulness and novelty in what we have done derives from putting these together in a script dedicated to the anlyses of images. (e.g. thresholding, centroid location), something which has definite application in the study of cell migration.

It enables the capacity to analyse murine myoblasts migration *in vitro* following gross cellular damage. Cells were capable of targeted migration towards the site of injury, covering on average 900 μm in a 48h period. The use of real time cell imaging illustrated that while little cell division occurred during the 48h period this alone did not account for the movement of the cells into the wound site. Having established both the model and the MATLAB™ programme, we next wished to utilise both to determine the processes underlying cellular migration of damaged C2 myoblasts in culture.

The use of pharmacological inhibitors of PI3K (LY294002) and MAPKK (PD98059) at the time of injury, suggests that both of these pathways have important roles to play in C2 cell migration following damage. Inhibition of PI3K culminated in a 50% reduction in cell migration over 48h, when compared with control cell migration. These data are supported by studies of Raftopolou and Hall [17, 30] who suggest that PI3K is involved in the development of cellular protrusions. In addition, in studies conducted in the *Diostelium* it has been demonstrated that the localisation of PI3K at the leading edge of the cell is linked with a restriction of PTEN activity to the rear of the cell, both of which appear to be key in migration [19, 31] . Finally and again in support of a role for PI3 kinase in myoblast migration, studies by Bandow et al. [32] illustrated that HGF facilitated myoblast migration was dependent on PI3 kinase activation. Furthermore, analysis using our purpose developed MATLAB™ program demonstrated that PI3K inhibition indeed affected the way in which the cells moved, with a decline not only in the total distance migrated, but also in the velocity of migration. At 24h post inhibition it appeared as if horizontal directionality was protected. Therefore, sustained PI3K activation over a 48h test period has implications not only for forward migration but also for speed of migration as illustrated through the addition of LY294002, which resulted in perturbed cellular migration directionality and an overall reduction in migration velocity. Importantly, however, while all of the above studies illustrate the important role that the PI3K signalling pathway plays not only in cellular migration, but more specifically also in myoblast migration, our data illustrate that other pathways must also be involved as the migrational capacity of the cells is only suppressed by 50% in the presence of LY 294002.

MAPK activation, in relation to cell migration, has received relatively little attention to date. Our results demonstrate that MAPK also has a positive role in regulating cell movement following damage. Inhibition of MAPK via application of PD98059 resulted in significantly attenuated migration velocity and directionality. Notably, under these conditions, there was no evidence of significant

myotube formation with addition of PD98059, as has previously been reported [33], suggesting that the migratory signals following damage are strong enough to over-ride cell differentiation signals, thus ultimately enabling tissue repair. Importantly, however, the current injury studies were performed in the presence of 20% serum and not under reduced serum conditions, where PD has been previously shown to enhance differentiation.

In support of a role of MAPK having a regulatory effect on cell protrusion development, Szczur and colleagues [34] studied mice null for the CDC42 regulator CDC42GTPase activating protein. They suggested that CDC42 mediates both migration and directionality via the MAPK pathway. This result leads to the suggestion that CDC42 plays an important role in the directionality and motility of migrating cells via a MAPK pathway [34, 35]. Furthermore, our findings offer support for the notion that MAPK activation (and although not assessed, potentially CDC42 activation) is necessary in order for a cell to be correctly orientated and to migrate effectively.

Our results demonstrate that MAPK and PI3Ks are candidates for regulating skeletal muscle cell migration. However, when each pathway was individually inhibited, migration was evident, suggesting cross talk between the two pathways, which can compensate for the individual inhibition. Indeed, when both MAP and PI3Ks were simultaneously inhibited, the effect on cell migration was catastrophic, resulting in significant inhibition of migration, which was associated with a visible decline in cellular protrusion formation as has been reported for both MAPK and PI3K inhibition [36, 37]. Using MATLAB™, we ascertained not only a drop in the directionality of cell movement, but also in the velocity of cell movement, thus offering further support for the multifunctional potential of these pathways and suggesting that MAP and PI3Ks play key and compensatory roles in skeletal muscle cell migration, following damage. Supporting these findings, it has been reported that the proposed cross-talk between PI3K and MAPK pathways is essential for effective glucose-induced vascular smooth muscle cell migration [36].

In conclusion, our results clearly extend and support the work of Hall [38, 39] and others [30, 37, 40] illustrating that there are key roles for both MAPK and PI3K within the mechanisms underlying directed skeletal muscle cell movement. The development of a new way of tracking individual cells as they migrate, will allow us to conclusively demonstrate the changes and modifications which occur to directed cell migration in response to muscle damage *in vitro*.

References

1 Tipton KD, Ferrando AA: Improving muscle mass: response of muscle metabolism to exercise, nutrition and anabolic agents. Essays Biochem 2008;44:85-98.

2 Mauro A: Satellite cell of skeletal muscle fibers. J Biophys Biochem Cytol 1961;9:493-495.

3 Petrella JK, Kim JS, Mayhew DL, Cross JM, Bamman MM: Potent myofiber hypertrophy during resistance training in humans is associated with satellite cell-mediated myonuclear addition: a cluster analysis. J Appl Physiol 2008;104:1736-1742.

4 Sinha-Hikim I, Cornford M, Gaytan H, Lee ML, Bhasin S: Effects of testosterone supplementation on skeletal muscle fiber hypertrophy and satellite cells in community-dwelling older men. J Clin Endocrinol Metab 2006;91:3024-3033.

5 Sinha-Hikim I, Roth SM, Lee MI, Bhasin S: Testosterone-induced muscle hypertrophy is associated with an increase in satellite cell number in healthy, young men. Am J Physiol Endocrinol Metab 2003;285:E197-205.

6 Carosio S, Berardinelli MG, Aucello M, Musaro A: Impact of ageing on muscle cell regeneration. Ageing Res Rev. 2011;10:35-42.

7 Peault B, Rudnicki M, Torrente Y, Cossu G, Tremblay JP, Partridge T, Gussoni E, Kunkel LM, Huard J: Stem and progenitor cells in skeletal muscle development, maintenance, and therapy. Mol Ther 2007;15:867-877.

8 Nobes CD, Hall A: Rho GTPases control polarity, protrusion, and adhesion during cell movement. J Cell Biol 1999;144:1235-1244.

9 Small JV, Anderson K, Rottner K: Actin and the coordination of protrusion, attachment and retraction in cell crawling. Biosci Rep 1996;16:351-368.

10 Torrente Y, El Fahime E, Caron NJ, Del Bo R, Belicchi M, Pisati F, Tremblay JP, Bresolin N: Tumor necrosis factor-alpha (TNF-alpha) stimulates chemotactic response in mouse myogenic cells. Cell Transplant 2003;12:91-100.

11 Glass DJ: Molecular mechanisms modulating muscle mass. Trends Mol Med 2003;9:344-350.

12 Glass DJ: Skeletal muscle hypertrophy and atrophy signaling pathways. Int J Biochem Cell Biol 2005;37:1974-84.

13 Keren A, Tamir Y, Bengal E: The p38 MAPK signaling pathway: a major regulator of skeletal muscle development. Mol Cell Endocrinol 2006;252:224-230.

14 Kramer HF, Goodyear LJ: Exercise, MAPK, and NF-kappaB signaling in skeletal muscle. J Appl Physiol 2007;103:388-395.
15 Yaffe D, Saxel O: A myogenic cell line with altered serum requirements for differentiation. Differentiation 1977;7:159-166.
16 Yaffe D, Saxel O: Serial passaging and differentiation of myogenic cells isolated from dystrophic mouse muscle. Nature 1977;270:725-727.
17 Raftopoulou M, Hall A: Cell migration: Rho GTPases lead the way. Dev Biol 2004;265:23-32.
18 Saini A, Nasser AS, Stewart CE: Waste management-Cytokines, growth factors and cachexia. Cytokine Growth Factor Rev 2006;17:475-486.
19 Chung CY, Funamoto S, Firtel RA. Signaling pathways controlling cell polarity and chemotaxis. Trends Biochem Sci 2001;26:557-566.
20 Sorci G, Riuzzi F, Arcuri C, Giambanco I, Donato R: Amphoterin stimulates myogenesis and counteracts the antimyogenic factors basic fibroblast growth factor and S100B via RAGE binding. Mol Cell Biol 2004;24:4880-894.
21 Stewart CE, Newcomb PV, Holly JM: Multifaceted roles of TNF-alpha in myoblast destruction: a multitude of signal transduction pathways. J Cell Physiol 2004;198:237-247.
22 Keenan TM, Hooker A, Spilker ME, Li N, Boggy GJ, Vicini P, Folch A: Automated identification of axonal growth cones in time-lapse image sequences. J Neurosci Methods 2006;151:232-238.
23 Entschladen F, Drell TL 4th, Lang K, Masur K, Palm D, Bastian P, Niggemann B, Zaenker KS: Analysis methods of human cell migration. Exp Cell Res 2005;307:418-426.
24 Thomas L, Byers HR, Vink J, Stamenkovic I: CD44H regulates tumor cell migration on hyaluronate-coated substrate. J Cell Biol 1992;118:971-977.
25 Smith A, Bracke M, Leitinger B, Porter JC, Hogg N: LFA-1-induced T cell migration on ICAM-1 involves regulation of MLCK-mediated attachment and ROCK-dependent detachment. J Cell Sci 2003;116:3123-3133.
26 Yarrow JC, Perlman ZE, Westwood NJ, Mitchison TJ: A high-throughput cell migration assay using scratch wound healing, a comparison of image-based readout methods. BMC Biotechnol 2004;4:21.
27 Mackarel AJ, Russell KJ, Brady CS, FitzGerald MX, O'Connor CM: Interleukin-8 and leukotriene-B(4), but not formylmethionyl leucylphenylalanine, stimulate CD18-independent migration of neutrophils across human pulmonary endothelial cells in vitro. Am J Respir Cell Mol Biol 2000;23:154-161.
28 Junkin M, Wong PK: Probing cell migration in confined environments by plasma lithography. Biomaterials;32:1848-1855.
29 He W, Halberstadt CR, Gonsalves KE: Lithography application of a novel photoresist for patterning of cells. Biomaterials 2004;25:2055-2063.
30 Raftopoulou M, Etienne-Manneville S, Self A, Nicholls S, Hall A: Regulation of cell migration by the C2 domain of the tumor suppressor PTEN. Science 2004;303:1179-1181.
31 Iijima M, Devreotes P: Tumor suppressor PTEN mediates sensing of chemoattractant gradients. Cell 2002;109:599-610.
32 Bandow K, Ohnishi T, Tamura M, Semba I, Daikuhara Y: Hepatocyte growth factor/scatter factor stimulates migration of muscle precursors in developing mouse tongue. J Cell Physiol 2004;201:236-243.
33 Al-Shanti N, Stewart CE: PD98059 enhances C2 myoblast differentiation through p38 MAPK activation: a novel role for PD98059. J Endocrinol 2008;198:243-252.
34 Szczur K, Xu H, Atkinson S, Zheng Y, Filippi MD: Rho GTPase CDC42 regulates directionality and random movement via distinct MAPK pathways in neutrophils. Blood 2006;108:4205-213.
35 Stewart AL, Young HM, Popoff M, Anderson RB: Effects of pharmacological inhibition of small GTPases on axon extension and migration of enteric neural crest-derived cells. Dev Biol 2007;307:92-104.
36 Campbell M, Allen WE, Sawyer C, Vanhaesebroeck B, Trimble ER: Glucose-potentiated chemotaxis in human vascular smooth muscle is dependent on cross-talk between the PI3K and MAPK signaling pathways. Circ Res 2004;95:380-388.
37 Campbell M, Trimble ER: Modification of PI3K- and MAPK-dependent chemotaxis in aortic vascular smooth muscle cells by protein kinase CbetaII. Circ Res 2005;96:197-206.
38 Hall A: Ras-related GTPases and the cytoskeleton. Mol Biol Cell 1992;3:475-479.
39 Hall A: Rho GTPases and the control of cell behaviour. Biochem Soc Trans 2005;33:891-895.
40 Leloup L, Daury L, Mazeres G, Cottin P, Brustis JJ: Involvement of the ERK/MAP kinase signalling pathway in milli-calpain activation and myogenic cell migration. Int J Biochem Cell Biol 2007;39:1177-1189.